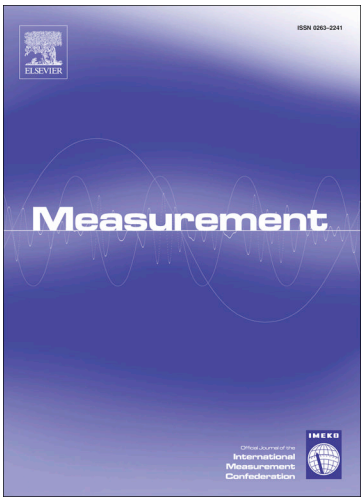

Smart Embedded Passive Acoustic Devices for Real-Time Hydroacoustic Surveys

Daniel Mihai Toma, Ivan Masmitja, Joaquín del Río, Enoc Martinez, Carla Artero-Delgado, Alessandra Casale, Alberto Figoli, Diego Pinzani, Pablo Cervantes, Pablo Ruiz, Simone Memè, Eric Delory

PII: S0263-2241(18)30411-1
DOI: https://doi.org/10.1016/j.measurement.2018.05.030
Reference: MEASUR 5531

To appear in: *Measurement*

Received Date: 29 January 2018
Revised Date: 30 April 2018
Accepted Date: 7 May 2018

Please cite this article as: D. Mihai Toma, I. Masmitja, J. del Río, E. Martinez, C. Artero-Delgado, A. Casale, A. Figoli, D. Pinzani, P. Cervantes, P. Ruiz, S. Memè, E. Delory, Smart Embedded Passive Acoustic Devices for Real-Time Hydroacoustic Surveys, *Measurement* (2018), doi: https://doi.org/10.1016/j.measurement.2018.05.030

Smart Embedded Passive Acoustic Devices for Real-Time Hydroacoustic Surveys

Daniel Mihai Toma[1], Ivan Masmitja[1], Joaquín del Río[1], Enoc Martinez[1], Carla Artero-Delgado[1], Alessandra Casale[2], Alberto Figoli[2], Diego Pinzani[2], Pablo Cervantes[3], Pablo Ruiz[3], Simone Memè[4], Eric Delory[4]

[1]*SARTI Research Group. Electronics Dept. Univeritat Politècnica de Catalunya, UPC Rambla Exposició 24, 08800, Vilanova i la Geltrú, Barcelona, Spain { daniel.mihai.toma, ivan.masmitja, joaquin.del.rio, enoc.martinez, carola.artero}@upc.edu*

[2]*SMID Technology srl Via Vincinella 12, Santo Stefano di Magra (SP), ITALY, {a.casale, a.figoli, d.pinzani}@smidtechnology.it*

[3]*Centro Tecnológico Naval y del Mar (CTN) Parque Tecnológico de Fuente Álamo, Ctra. El Estrecho-Lobosillo, km.2, 30320, Fluente Álamo (Murcia), Spain {pablocervantes, pabloruiz}@ctnaval.com*

[4] *Plataforma Oceánica de Canarias (PLOCAN), Carretera de Taliarte s/n, 35200, Telde, Gran Canaria, Spain {simone.meme, eric.delory}@plocan.eu*

***Abstract* – This paper describes cost-efficient, innovative and interoperable ocean passive acoustics sensors systems, developed within the European FP7 project NeXOS (Next generation Low-Cost Multifunctional Web Enabled Ocean Sensor Systems Empowering Marine, Maritime and Fisheries Management) These passive acoustic sensors consist of two low power, innovative digital hydrophone systems with embedded processing of acoustic data, A1 and A2, enabling real-time measurement of the underwater soundscape. An important part of the effort is focused on achieving greater dynamic range and effortless integration on autonomous platforms, such as gliders and profilers. A1 is a small standalone, compact, low power, low consumption digital hydrophone with embedded pre-processing of acoustic data, suitable for mobile platforms with limited autonomy and communication capability. A2 consists of four A1 digital hydrophones with Ethernet interface and one master unit for data processing, enabling real-time measurement of underwater noise and soundscape sources. In this work the real-time acoustic processing algorithms implemented for A1 and A2 are described, including computational load evaluations of the algorithms. The results obtained from the real time test done with the A2 assembly at OBSEA observatory collected during the verification phase of the project are presented.**

Keywords – underwater acoustics; digital hydrophone; interoperability; marine observations; smart interface; embedded processing, underwater noise, bioacoustics

1. Introduction

More than 70% of the earth's surface is covered by oceans and the majority of the underwater space remains unexplored. Because in-situ observation of oceans is generally difficult and costly in resources and time, the NeXOS project developed innovative, cost-effective, and compact multifunctional sensor systems for a number of domains and applications, including ocean passive acoustics, ocean optics and for an Ecosystem Approach to Fisheries (EAF). These systems were envisioned to be deployed both from mobile and fixed platforms, with data services contributing to the Global Earth Observing System of Systems (GEOSS), the Marine Strategy Framework Directive (MSFD) and the Common Fisheries Policy of the European Union [1].

Passive Acoustic Monitoring (PAM) systems are extremely valuable for long term studies of the marine environment, for example, information on species occurrence and temporal distribution can be gathered using passive acoustics before and after anthropogenic activity begins. PAM in areas of

such human activities can be an effective way to monitor how noise potentially affects marine mammals by measuring how much of their acoustic habitat is being lost [2]. Generally, PAM systems include: single or multiple acoustic transducers for sound acquisition; internal electronics to control the system and for acoustic data conditioning, storage of raw audio data [3], and some may provide processing power to analyse acoustic data in real-time [4][5]. However, the majority of the available commercial passive acoustic sensors cannot perform simultaneous measurement of sound level extremes (very low and very high), and data processing has to be performed on costly and/or bulky systems, generally impractical for mobile platforms [3].

Hence, in addition to acquiring raw audio data, the NeXOS passive acoustic devices have been envisioned to enable the provision of information for the assessment of underwater noise, marine mammal populations, detection of fish reproduction areas, detection of Green-House Gases (GHG) seepage from pipelines and deep sea carbon storage, gasification of methane clathrates, estimation of rainfall, detection of low-frequency seismic events, ice-cracking, ocean basin thermometry and tomography, acoustic communication, etc. [6]. From a technical perspective, the focus is on improved life cycle cost-efficiency via the implementation of innovations, such as multiplatform integration, greater reliability through better antifouling management and greater sensor and data interoperability. Requirements for the sensors have been refined from this perspective through surveys and discussions with science and industry users. The feedback has then been incorporated into the engineering design process.

Within this context, we developed and implemented new, compact, low power and innovative digital hydrophones, that we describe in this paper. These passive acoustic sensors can be arranged in different configurations: as a standalone multi-channel hydrophone (named A1) or as a hydrophone array (named A2). First, an overview of the challenges for real-time hydroacoustic surveys with embedded passive acoustic devices is presented. Section 2 focuses on the design philosophy of the standalone multi-channel hydrophone (A1) and the hydrophone array (A2), including the description of the two devices, three hydrophone transducers used in the final development, and multiplatform interoperability. In Section 3 the algorithms implemented for the assessment of the underwater noise (MSFD Descriptor 11), mammal detection (MSFD Descriptor 1) and sound source localization are detailed. During the validation and demonstration phase various deployments of the A1 hydrophone have been carried out with deferent platforms such as gliders, profilers and buoys, and a deployment of A2 hydrophone array in OBSEA observatory which are discussed in Section 4. Finally, the conclusions drawn are presented in Section 5.

2. Passive acoustic sensors system

2.1. A1 Hydrophone

The A1 is a dual-channel compact, low-power digital hydrophone aimed to be deployed on mobile platforms. In order to extend its dynamic range, it has two channels with different gain, sampled simultaneously enabling it to detect acoustic source levels from 50 dB to 180 dB re 1µPa in the frequency range from 1Hz to 50 kHz. Considering the inherent sensitivity of hydrophone transducers, the use of two amplifier stages with different gains is a cost-efficient approach in order to obtain the desired dynamic range.

As illustrated in Figure 1, as a first step, the hydrophone signal is pre-amplified with an input stage with a gain of 20 dB. The first channel (CHA) consists of a high pass filter “equalizer”, connected before the high gain stage in order to avoid saturation at low frequency caused by rough sea, ship traffic, etc. The equalizer circuit is a one-pole filter with a cut-off frequency of 3200 Hz which can be enabled or disabled through the serial interface. Furthermore, the equalizer also ensures high

dynamic range at high frequency, where the ambient noise level is lower. The post gain amplifier of CHA can be set to 20 dB or 40 dB through the MCU. The second channel (CHB) does not make changes to the hydrophone's pre-amplified signal. Therefore, the two channels provide different gain:

- CHA "Hi" Gain: 40 dB or 60 dB
- CHB "Low" Gain: 20 dB

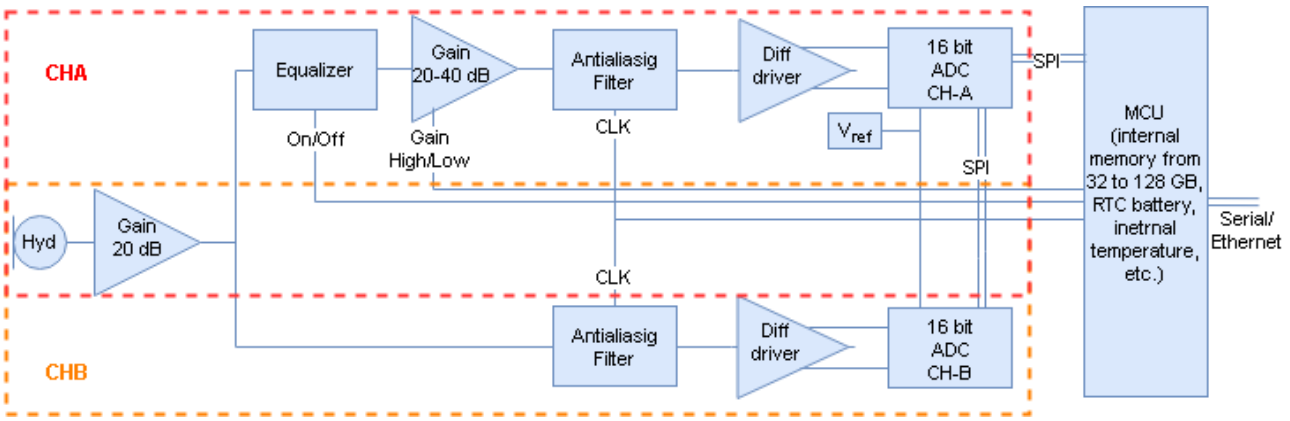

Figure 1 A1 sensor block diagram. CHA is demarcated in red and CHB is demarcated in orange.

Both channels have a low pass antialiasing filter: to avoid aliasing problems, a switched capacitor filter, digitally controlled by the MCU, has been added in both the chains after the amplifier stage. The operator, through the MCU, can set the cut off frequency of the anti-aliasing filter, changing its control clock frequency (CLK), depending on the application and on the sampling frequency. The hydrophone signal is sampled by two 16-bit SAR converters controlled by an ARM microcontroller, which is responsible for proper data processing (mathematical operations). The working sampling frequency (SF) should be 100 Kilo Samples Per Second (KSPS) and it is controlled by the MCU timer.

The MCU processes the sampled data and transmits the results on an EIA RS-232 serial port. A1 is equipped with a Real-Time Clock (RTC) with a precision of ±3.5ppm and powered by an RTC battery, useful to tag temporally sampled data, but it is also equipped with a Pulse Per Second (PPS) input for the GPS link, if available. The frequency response requirement is a frequency range of 1Hz to 50 kHz. The selected ADC can run up to 100 KSPS (50 kHz of bandwidth). Any frequency range may be selected by the MCU by changing the antialiasing filter frequency clock.

The A1 Hydrophone can acquire raw acoustic data and store it in its internal memory (128 GB). However, it also has several embedded processing algorithms, which permit real-time measurements of Sound Pressure Level (SPL), click detection, whistle detection and low frequency tonal sounds detection. Regarding the transducer stage, three types of hydrophones, SQ26-01, D/70 and JS-B100 (see Table 1) have been selected for the final developments as illustrated in Figure 2. The maximum power consumption of the A1 hydrophone is approximately 920 mW in running mode and 36 mW in sleep mode.

Figure 2 A1 hydrophone with JS-B100 acoustic transducer

2.2. A2 Hydrophone Array

The A2 Hydrophone Array is a digital passive acoustic transducer array whose output (raw signal) is pre-processed by a master unit. The acoustic array consists of four slave acoustic devices, called A2 hydrophones, and a master unit, based on an embedded Linux computer. The A2 slave hydrophones have the same characteristics as the A1 sensor regarding the Signal Conditioning Unit (SCU), the A/D Converter (ADC) and the Micro Controller Unit (MCU), with the difference of a smaller internal memory (32 GB) and the absence of the RTC battery. Regarding the transducer stage, the JS-B100 has been selected (see Table 1) to permit high depth underwater application. The maximum power consumption of the A1 hydrophone is approximately 1.12 W in running mode and 36 mW in sleep mode.

The time synchronization of the master unit and the slave units (A2 hydrophones) is accomplished by implementing the IEEE1588 Precision Time Protocol (PTP) standard [7]. This standard defines a network protocol enabling accurate and precise synchronization, below microseconds, of the real-time clocks of devices in networked distributed systems. Therefore, A2 array is composed of four hydrophones A2 hydrophones, a PTP Grandmaster Clock plus one Master Unit; Figure 3 shows the block diagram of the A2 hydrophone array.

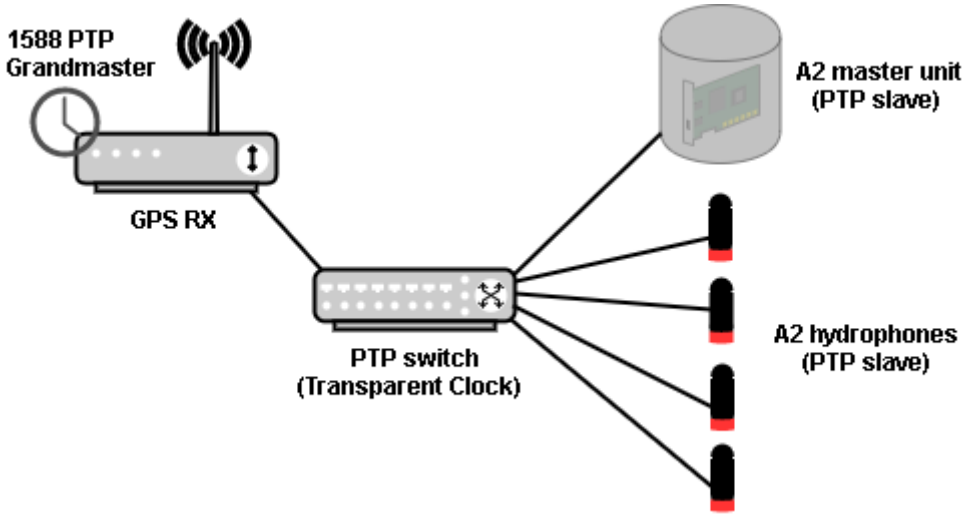

Figure 3 Block diagram of A2 hydrophone array with Master Unit and PTP Components

The A2 Hydrophone Array can be equipped with positioning sensors (pan, tilt, and compass) to allow the measurement of its geo-referenced position. The device can also receive relevant oceanographic parameters (sound velocity, temperature, depth, time) via Ethernet, in order to optimize the algorithms. Therefore, the main capability of A2 is to provide directional sound source information for hydroacoustic surveys.

2.3. Hydrophone Transducers

Within the NeXOS project context, three types of transducers suitable for A1 and A2 sensor system requirements have been identified. Differences consist in sensitivity, shape, maximum operating depth and cost. A comparison between the transducers is shown in Table 1. A prototype of A1 was manufactured for each of these transducers and a prototype of A2 was manufactured for JS-B100 transducer.

Table 1 Characteristics of NeXOS hydrophones based on the three types of transducers

Transducer Type &Specifications	**Technology Limited mod. SQ26-01**	**Neptune Sonar mod. D/70**	**JS-B100-C4DP Acoustic Sensor**
Sensitivity CHA	-133.5/-153.5 dB	-138/-158 dB	-141/-161 dB
Sensitivity CHB	-173 dB	-178 dB	-181 dB
Frequency range (±1.5dB)	From .151 Hz to 28 kHz	From 1 Hz to 50 kHz	From 1 Hz to 50 kHz
Input equivalent Noise (@5kHz G=60dB	22.5 dB re 1 µ Pa/ √ Hz	27 dB re 1 µ Pa/ √ Hz	30 dB re 1 µ Pa/ √ Hz
Beam pattern	Omni-directional	Omni-directional	Omni-directional

Working depth	Up to 2000 m	Up to 1500 m	Up to 3600 m
Weight	317 g	333 g	480 g
Size	Φ34X255mm	Φ34X255mm	Φ34X255mm

2.4. Gain and equalizer configuration

As shown in the table below, the architecture of the hydrophone is conceived and designed to allow many different working configurations, selectable via software.

Table 2 Gain and Equalizer configurations

Configuration	**Acquired channel**	**Gain state (CHA ON/OFF =60/40 dB gain)**	**Equalizer state**
1a	A and B	ON	OFF
1b	A and B	OFF	OFF
2	A	ON	OFF
3	A	OFF	ON
4	B	OFF (recommended)	ON (recommended)

The configuration 1a and 1b allows both CHA and CHB to be acquired making it possible to achieve NeXOS dynamic range requirements to measure an acoustic pressure level from 50 to 180 dB re µPa. The configuration 1b is activated when the CHA is in saturation condition. Configuration 2 should be used only in quiet sea conditions, especially in deep water. This implies a reduction of power processing consumption. Configuration 3 activates the one-pole high pass filter, which works with the intermediate gain of CHA of 40dB. It can be used in the presence of low frequency noise generated by ship traffic and by bad weather conditions. Configuration 4 is recommended only at low frequencies, where sea noise is higher than self-noise. It can be used as a seismic hydrophone in low frequency range. Selecting the intermediate gain of CHA of 40dB and turning on the equalizer in order to decrease crosstalk interferences on the adjacent CHB is recommended. This implies a reduction of electronic power consumption.

2.5. Multiplatform Interoperability

Within the NeXOS project, special emphasis has been laid on the sensor interoperability and multiplatform integration. Therefore, the use of the Open Geospatial Consortium's (OGC) Sensor Web Enablement (SWE) framework has been adopted. This set of protocols and standards provides a well-defined framework to acquire, archive and share sensor data and metadata among intelligent nodes [8]. To facilitate their integration into SWE-based data infrastructures, the A1 and A2 hydrophones implement the Smart Electronic Interface for Sensor Interoperability (SEISI) [9].

From the instrument side, the SEISI interface implements OGC-PUCK protocol, allowing automatic instrument detection and identification without any a priori knowledge of the instrument [10]. Furthermore, this protocol also permits data to be embedded in a memory within the instrument itself. This memory is used to store instrument metadata encoded according to the Sensor Model Language (SensorML) standard [11]. Each sensor, platform and actuator developed within the project has its own SensorML description facilitating sensor identification and data traceability. Furthermore, within its SensorML, the whole command interface can be described. Therefore, a PUCK-capable platform can automatically access and interpret this metadata, providing plug and play capabilities. [12]

A1 and A2 integrate OGC-PUCK with SensorML metadata embedding interface command description, enabling sensor status traceability and providing plug and play capability for PUCK capable platforms [13], [14]. The SensorML provided inside each system in the PUCK payload (as shown in Figure 4), can be reconfigured for each new deployment, in any scenario, by the observatory operator or by the scientist [15].

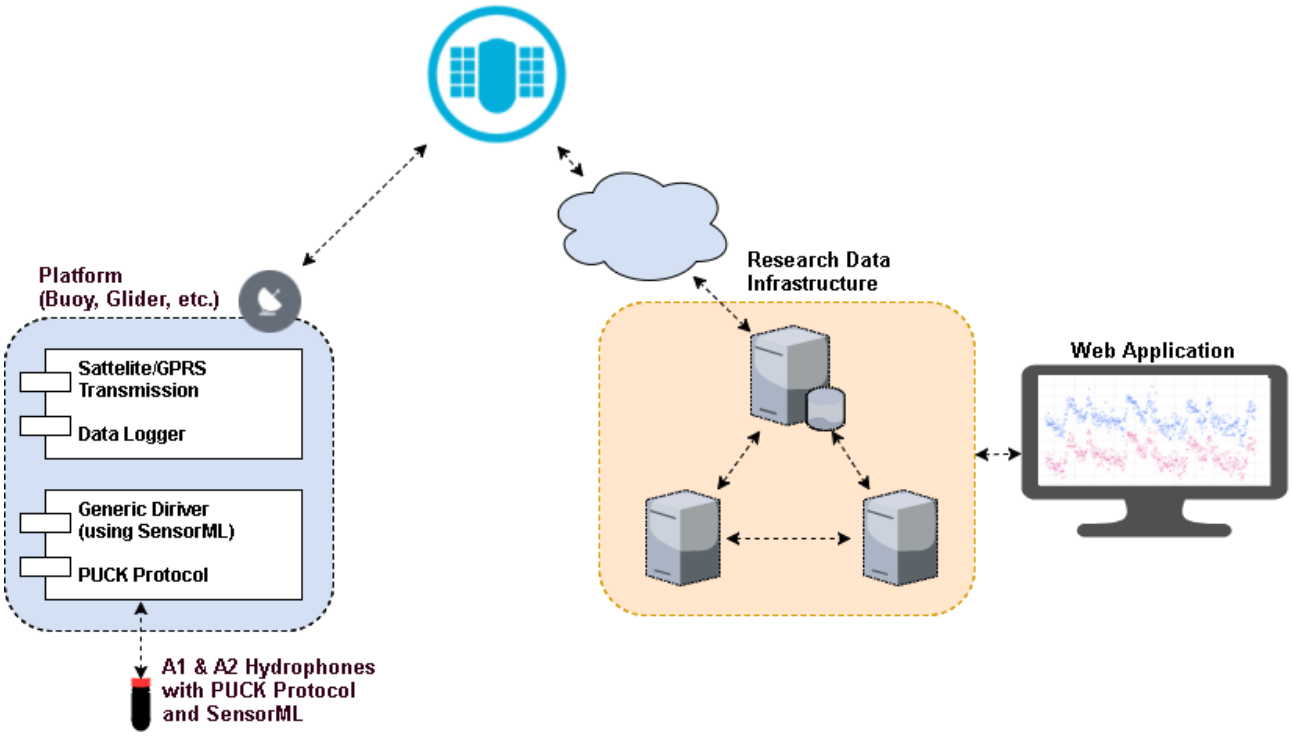

Figure 4 Standard processes between Marine Sensor Web architecture and components and the A1 and A2 hydrophones

The SensorML description provides the configuration for the platforms where A1 or A2 hydrophones are deployed. The host can then use the information from the SensorML inside the PUCK payload to automatically configure the operation mode, i.e. sampling period, auto-manage new sensors connected to its input interfaces, enable output interface (Ethernet, Serial), IP filters, etc.

From the web side, a driving factor behind the design of the Sensor Web architecture is the provision of a cost-efficient solution that allows data providers to integrate their sensors and sensor data easily into a web-based infrastructure [16]. This aim of a cost-efficient approach is achieved through several characteristics of the architecture: Re-Usability, Interoperability (through the use of international standards) and Open Source.

3. Signal Processing

A1 Hydrophone implements signal processing algorithms in order to provide the capabilities, including tracking, measuring and classifying features, relevant to MSFD Descriptor 11 (Energy/Underwater Noise) and Descriptor 1 (Biodiversity) for the A1 hydrophone, as depicted in Figure 5.

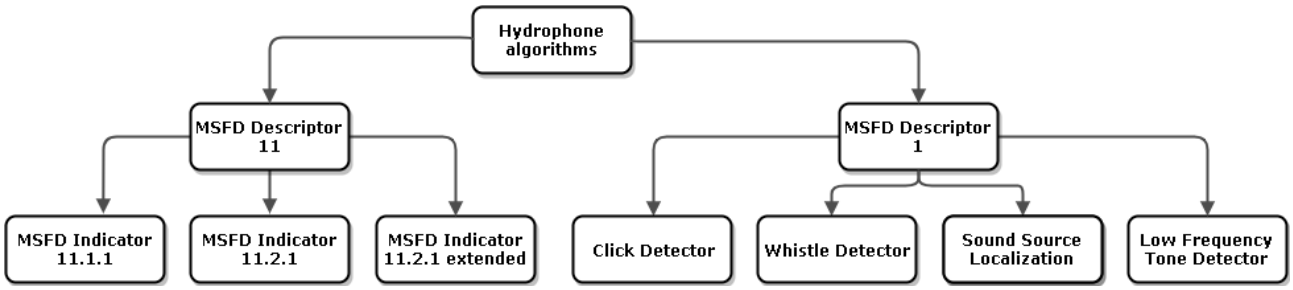

Figure 5 MSFD indicators covered by the algorithms implemented in A1 hydrophone

3.1. MSFD Descriptor 11

For the MSFD Descriptor 11, three different algorithms have been developed taking into account the MSFD requirements regarding Indicator 11.2.1 and Indicator 11.1.1 [17], [1] and [18]. As shown in Figure 6, the output of the algorithms for the MSFD Descriptor 11 implemented in the A1 hydrophone are the ***Total SPL_{rms}*** and ***Percentile Levels*** described as:

- ***Total SPL_{rms}***: the SPL_{rms} is computed as stated in (1), corresponding to a period of integration time (T) defined by the user.

$$SPL_{rms} = 20\ log_{10}\left(\sqrt{\frac{1}{T}\int_{T} P(t)^2\ dt}\right) \qquad (1)$$

- ***Percentile Levels***: They are very useful parameters to obtain knowledge about maximum levels and background noise discarding spontaneous and unusual SPL levels. According to [29], N percent exceedance level is the time-weighted and frequency-weighted sound pressure level that is exceeded for N % of the time interval considered. It is also mentioned that "Residual sound may be approximated by the percentile sound level exceeded during 90 – 95 % of the measurement period". Since there are no general recommendations for the use of percentile parameters, we have decided to calculate L_{10} and L_{90} as the level that is exceeded 10 and 90 times out of 100, in order to offer information about maximum and background noise present in the measurement. Therefore, the L_{10} represents the level that has been exceeded 10 % of the time. Consequently, it will be close to the peak level. The L_{90} represents the level that has been exceeded 90 % of the time. Therefore, it will be close to the background noise. However, these percentile levels can be changed by the user, and any percentage can be calculated and stored for its analysis.

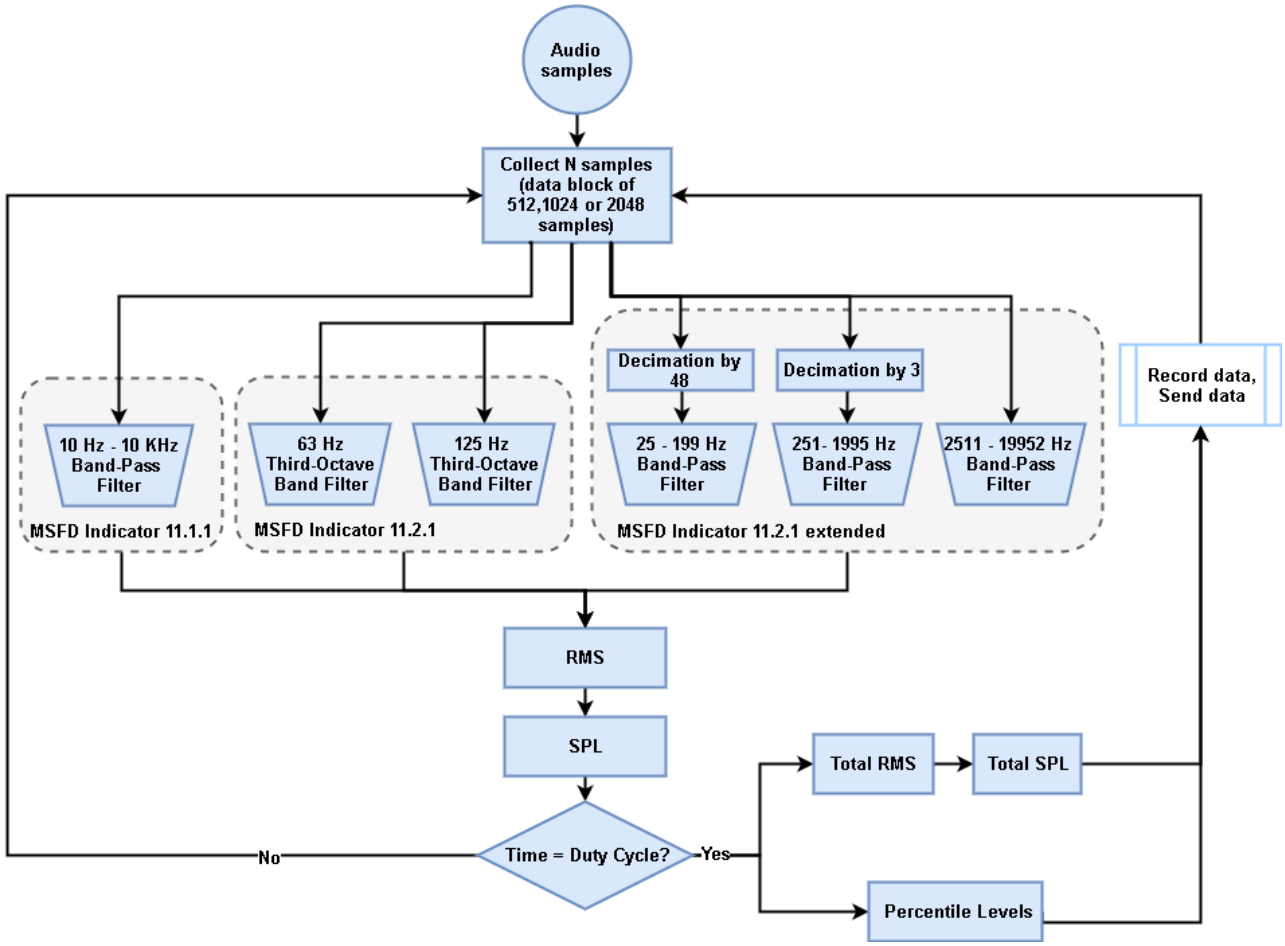

Figure 6 Block diagram of the algorithms used to compute the Indicators for Descriptor 11using the A1 hydrophone

3.1.1. MSFD Indicator 11.1.1

The MSFD Indicator 11.1.1 is described as the proportion of days and their distribution within a calendar year over areas of a determined surface, as well as their spatial distribution, in which anthropogenic sound sources exceed levels that are likely to entail significant impact on marine animals measured as Sound Exposed Level (in dB re 1 µPa 2. s) or as peak sound pressure level (in dB re 1 µPa peak) at one metre, measured over the frequency band 10 Hz to 10 kHz [19]. Therefore, the implementation of the present algorithm in A1 hydrophone is performed based on a 10 Hz to 10 kHz band-pass filter. The purpose of this indicator is to assess the pressure on the environment by making an overview of all low and mid-frequency impulsive sound sources available over a period of one year throughout regional seas. This algorithm is able to filter out an input acoustic data and extract the ***Total SPL***$_{rms}$ and ***Percentile Levels*** measured over the frequency band 10 Hz to 10 kHz.

3.1.2. MSFD Indicator 11.2.1

According to the Technical Subgroup on Noise (TSG), the MSFD Indicator 11.2.1 should provide trends in the annual average of the squared sound pressure associated with ambient noise in each of the two third octave bands, one centred at 63 Hz and the other centred at 125 Hz, expressed as a level in decibels, in units of dB re 1 µPa, either measured directly at observation stations, or inferred from a model used to interpolate between, or extrapolate from, measurements at observation stations. As depicted in Figure 6, two filters are needed to meet the requirements of the Indicator 11.2.1. This algorithm is able to filter out an input acoustic data and extract the ***Total SPL***$_{rms}$ and

Percentile Levels measured in each of the two third octave bands, one centred at 63 Hz and the other centred at 125 Hz.

3.1.3. Extended MSFD Indicator 11.2.1

The algorithm for the extended MSFD Indicator 11.2.1 is an addition of the MSFD Indicator 11.2.1. While the Indicator 11.2.1 calculate the trends in the ambient noise level within 1/3 octave bands 63 and 125 Hz, in the extended Indicator 11.2.1, the range of ambient noise level calculated is substantially increased from 20 Hz to 20 KHz. According to IEC 61260 [20], the number of third-octave bands within the frequency range (20 – 20 KHz) is 30. Therefore, a total of 30 filters are applied to the input signal in order to obtain the SPL_{rms} corresponding to each frequency band. The number of decimation orders has been minimized obtaining a total of 3 different orders. Decimation, which is needed here due to filtering implementation constraints of the processing platform, is the process of decreasing the sampling frequency of a given signal. Therefore, after the decimation process by 2 different orders (48 and 3), 2 different new sampling frequencies will be obtained. A FIR filter of order 100 is used for the decimated signal. For filters with a sampling frequency of 1000 Hz, a decimation factor of 48 is used. For filters with a frequency of 16000 Hz, a factor of 3 is used and for the filters with sampling frequency of 48 KHz, no decimation factor is used. The sampling frequency of the input has to be 48 kHz, so the sampling frequencies obtained from the decimation process are 1 kHz and 16 KHz. Each of these sampling frequencies are used for the signal to be filtered in different frequency ranges as depicted in Figure 6. This algorithm is able to filter out an input acoustic data and extract the ***Total SPL_{rms}*** and ***Percentile Levels*** measured over the frequency band 25 Hz to 199Hz, frequency band 251 Hz to 1995Hz and frequency band 2511 Hz to 19952Hz.

The graph below shows the computational load of the different algorithms running on A1 hydrophone for the MSFD Descriptor 11 with different duty cycles and a data block of 2048 samples. The sampling rate used to acquire the audio data is 1000Hz for MSFD Indicator 11.2.1 and 48000Hz for MSFD Indicator 11.1.1 and extended MSFD Indicator 11.2.1.

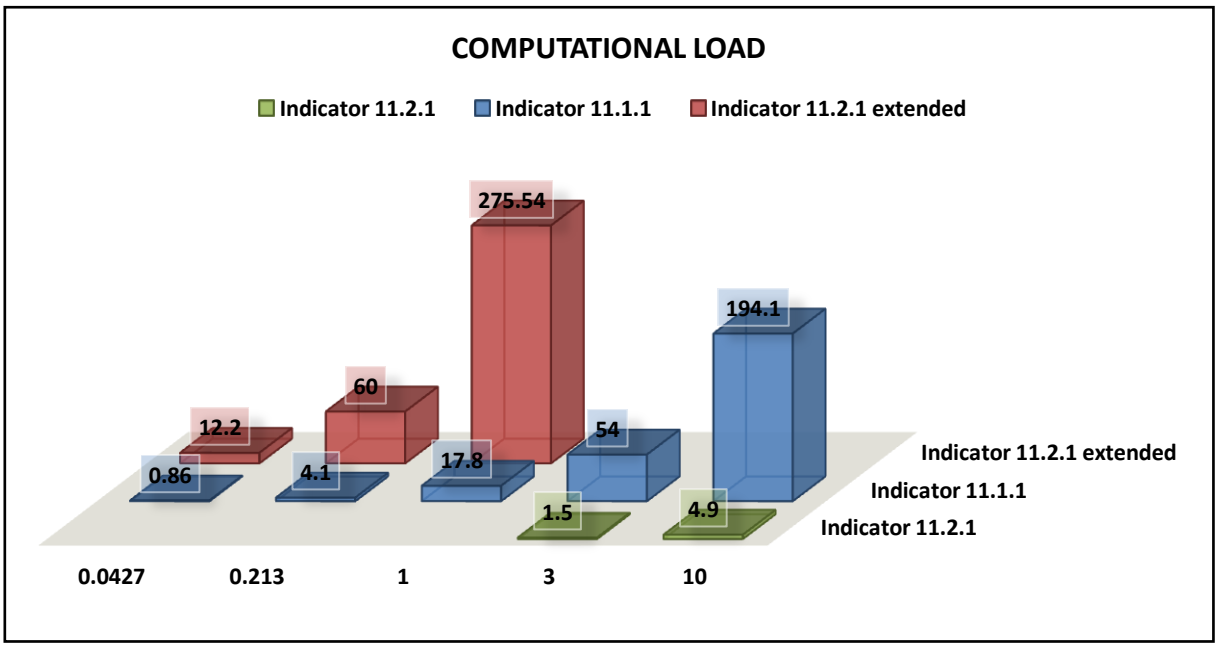

Figure 7 Computational time in milliseconds of the three algorithm with different duty cycles [0,0427s; 0,213s; 1s; 3s; 10 s]

Each block of 2048 samples takes around 1.5 msec. for MSFD Indicator 11.2.1, 0.86 msec. for MSFD Indicator 11.1.1 and 12.1 msec. for extended MSFD Indicator 11.2.1 at a sampling rate of 48000Hz. The algorithms are fast enough to be executed in real time, however, the algorithm for extended MSFD Indicator 11.2.1 is about 10 times slower because it has many more filters to compute. Therefore, the algorithm for extended MSFD Indicator 11.2.1 can only be executed for duty cycles of maximum 1 second.

3.2. MSFD Descriptor 1

Based on the review of reference passive acoustic detection techniques [6], three different algorithms have been implemented in A1 hydrophone for the MSFD Descriptor 1 (Click Detector, Whistle Detector and Low Frequency Tonal Sounds). The first two algorithms are based on the community-developed open-source software PAMGuard and the third is based on the work published by Zaugg et. al. [17], [21] .

3.2.1. Click Detector

The Click Detector algorithm implemented on A1 hydrophone is based on the Java implementation of the click detector that can be found on the PAMGuard source code [21]. This algorithm has been redesigned and optimized to be implemented on the A1 embedded platform. Its main purpose is to distinguish a click within the input signal. When this algorithm is selected, the sampling frequency of the A1 hydrophone is set at 100 kHz as it is considered the best sampling frequency for click detection.

This algorithm consists of a trigger filtering stage, a trigger decision module, localization and peak level module. The purpose of the trigger filtering stage is to increase the efficiency of the click detection by letting just the information related to the marine animal vocalization be introduced into the trigger decision module.

Next, the trigger decision module automatically measures background noise and then compares the signal level to the noise level. When the signal level reaches a certain threshold above the noise level, a click clip is initiated. When the signal level falls below the threshold for more than a set number of bins, the click clip is ended and the clip is sent to the localization modules. The trigger decision stage is able to detect and extract relevant information about the click detected. This information consists of: time localization of click event, $Lpeak$- maximum SPL in frequency and the main frequency (Hz), which is the frequency of maximum amplitude. Special attention has been paid to the triggering filtering stage and the specification of the threshold level, which has to be referenced to 1 μPa.

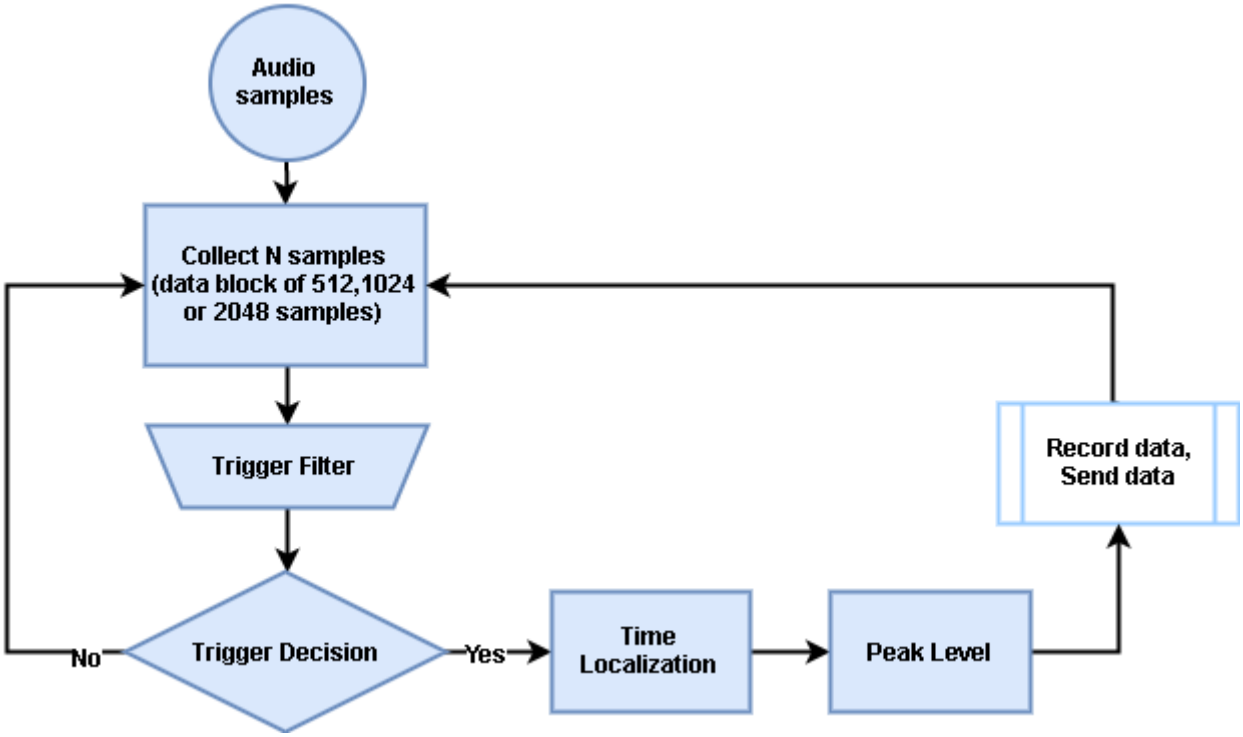

Figure 8 Block diagram of the algorithms used to compute the Click Detector using the A1 hydrophone

3.2.2. Whistle Detector

The algorithm is based, like the Click Detector algorithms, on the open source software PAMGuard [21]. When this algorithm is selected, the sampling frequency of the A1 hydrophone is set at 48 kHz. Although the whistle detector works properly at any sampling frequency, higher sampling frequency will need more bandwidth. As illustrated in Figure 9, the algorithm consists of a spectrogram stage, a median filter, an average subtraction stage, a threshold stage and a connection region module.

The spectrogram consists of successive FFTs of the data input, with a determined number of points and a determined FFT hop, which overlaps one slice with another. This overlap is configured here via a parameter called FFT_{hop}. This parameter indicates the jump from the beginning of a FFT and the beginning of the next one. A typical FFT_{hop} is 50 % of the FFT_{length} parameter where FFT_{length} is the number of samples processed.

The median filter is implemented to enhance tonal peaks in the spectrogram by flattening the spectrum across the entire frequency range. In order to do this, it uses the median value to obtain stable values for the central tendency of each whistle.

The aim of the average subtraction module is to remove constant tones from the spectrogram by running average background removals to eliminate constant tones and subtracting them from the output of the median filter. Next, a threshold is applied to the output of the average subtraction module, putting all data points in the de-noised spectrogram below a defined threshold set to zero.

Finally, the connection region module connects the points in the spectrogram proceeding from the threshold stage to define the regions with whistles detected. This block has two possible outputs: one in which the points of the de-noised spectrogram over the threshold are set to 1, and the other in which those points are left with their FFT values. The binary map of points proceeding from the

threshold is divided into regions according to whether the pixels are in touch or not. Parameters such as minimum total length or minimum number of pixels determine when a region is considered a whistle or is discarded.

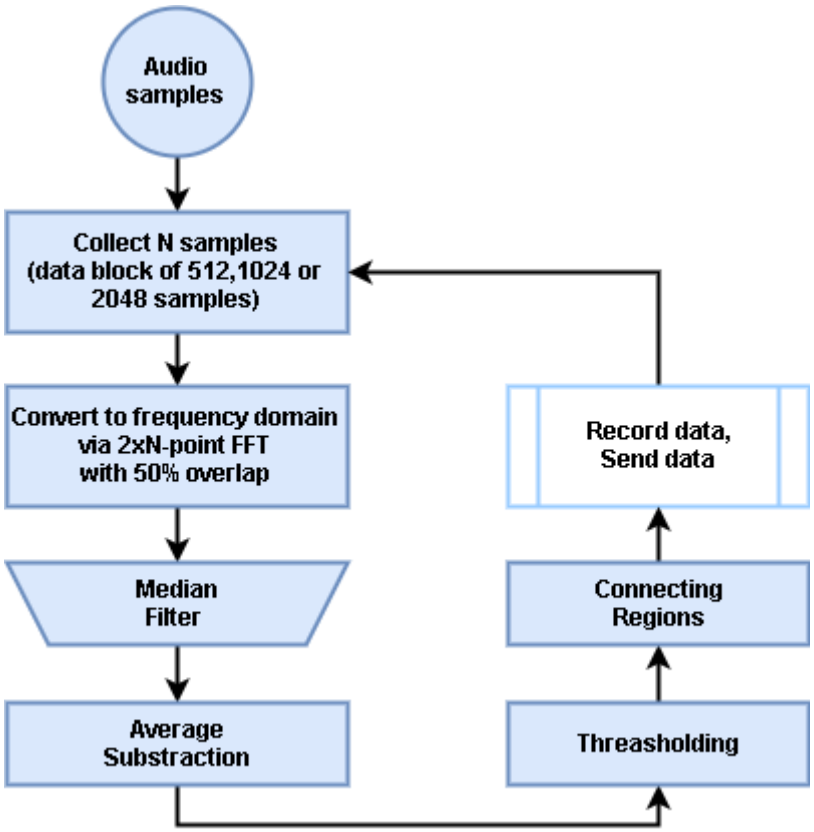

Figure 9 Block diagram of the algorithms used to compute the Whistle Detector using the A1 hydrophone

3.2.3. Low Frequency Tonal Sounds

Low frequency tone detector aims to detect short tonal sounds at low frequencies. This algorithm is based on the algorithm described by Serge Zaugg et.al.[13]. When this algorithm is selected, the sampling frequency of the A1 hydrophone is set at 48 kHz, as the low frequency tones are expected to be below 10 kHz.

As illustrated in Figure 10, the algorithm consists of a spectrogram stage, a median filter, an equalisation stage, a raw toneless peak stage and a thresholding module. In the spectrogram stage, the algorithm obtains the power spectrum of the input by means of the FFT with a Hanning window. The equalisation module performs an equalization to remove variation in the spectra due to background noise. Next, the raw tonalness peak module obtains a raw tonalness peak for each time bin. Finally, the thresholding stage compares the signal obtained in the previous module with a certain threshold. If the signal is above it, a low frequency tone is detected.

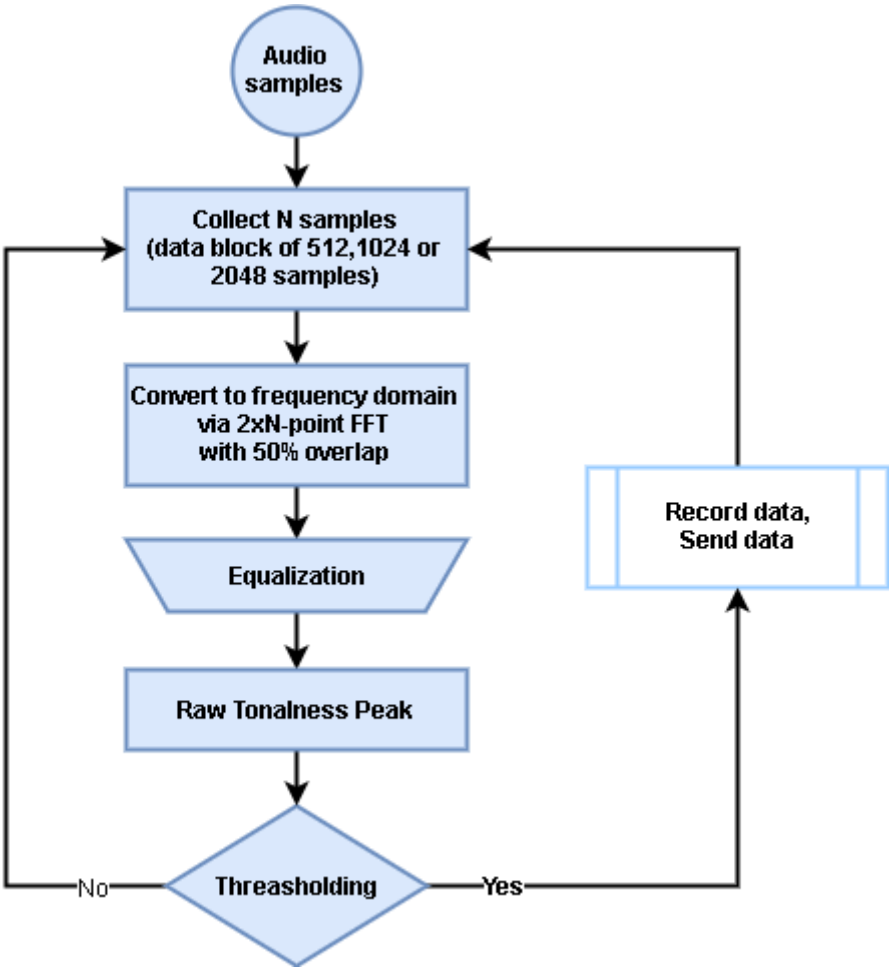

Figure 10 Block diagram of the algorithms used to compute the Low Frequency Tone Detector using the A1 hydrophone

3.3. Sound Source Localization

The algorithm for sound source localization implemented in the A2 array configuration depicted in Figure 11 has been developed based on the original method using the Time Difference Of Arrival (TDOA) estimation [22].

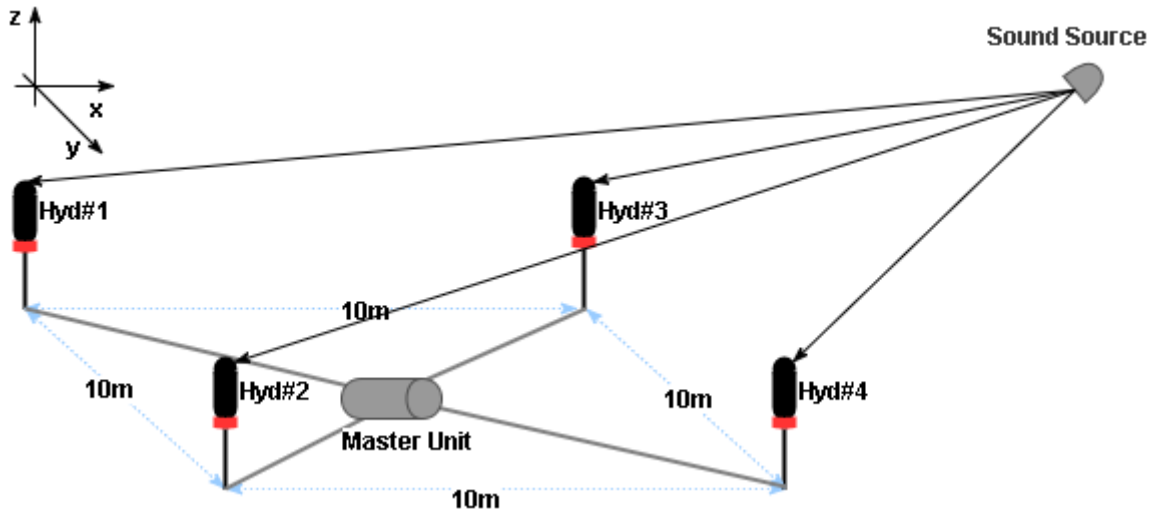

Figure 11 A2 array configuration for 2D localizations

As depicted in 11, the master unit is considered as the origin of coordinates of the Cartesian coordinate system arranged by the 4 hydrophones. In this configuration, the 4 hydrophones are placed on the same plane, generally the seabed. The Direction Of Arrival (DOA) of a source sound is characterized by two angles, the azimuth (ϕ) and the elevation (θ). The DOA estimation deals with the case where the source is in the array's far-field, which is equivalent to a plane wave at the sensor array [23]. With this assumption, we can consider the unit vector at the sensor array pointing towards the source as

$$\boldsymbol{a}_{\theta,\phi} = \boldsymbol{a}_{DOA} = [-sin\theta\cos\phi \quad -sin\theta\sin\phi \quad -cos\theta]^T . \tag{2}$$

The TDOA of the source signal from each hydrophone pair ij is defined as τ_{ij}, and corresponds to the estimated time required for the sound wavefront coming in the direction of $\boldsymbol{a}_{\theta,\phi}$ to travel a distance d_{ij} [24], given by

$$d_{ij} = \boldsymbol{a}_{\theta,\phi}^T(\boldsymbol{p}_i - \boldsymbol{p}_j), \tag{3}$$

where $\boldsymbol{p}_i$ and $\boldsymbol{p}_j$ are the position vectors of two sensor array elements. Moreover, the d_{ij} can be computed under far-field assumption as

$$d_{ij} \simeq \hat{\tau}_{ij}\, c, \tag{4}$$

where c is the sound speed in water. Equations (2), (3) and (4) can be written in a linear matrix form $\boldsymbol{Ax} = \boldsymbol{B}$, where

$$\boldsymbol{A} = \Delta\boldsymbol{p} = \begin{bmatrix} (p_{ix} - p_{jx}) & (p_{iy} - p_{jy}) & (p_{iz} - p_{jz}) \\ \vdots & \vdots & \vdots \\ (p_{ix} - p_{nx}) & (p_{iy} - p_{jy}) & (p_{iz} - p_{nz}) \end{bmatrix}, \tag{5}$$

$$\boldsymbol{x} = \boldsymbol{a}_{DOA} = \begin{bmatrix} a_x \\ a_y \\ a_z \end{bmatrix}, \tag{6}$$

$$\boldsymbol{B} = \boldsymbol{d} = \begin{bmatrix} d_{ij} \\ \vdots \\ d_{in} \end{bmatrix}, \tag{7}$$

where n is the number of hydrophone pairs. Using a minimum of three sensors in a 2D scenario, and four or more sensors in a 3D scenario, knowing the TDOA, and the sensor array position, the $\boldsymbol{a}_{DOA}$ is uniquely determined, with full-rank matrix where all equations are linearly independent, and can be computed in a closed-form solution, directly or using a least squares method for overdetermined systems [25]. Finally, from (6) and using the definition in (2), we can estimate the azimuth angle as $\hat{\phi} = tan^{-1}(\hat{a}_y/\hat{a}_x)$ and the elevation angle is given by $\hat{\theta} = cos^{-1}(-\hat{a}_z)$ as in [26].

The algorithms shown in Figure 12 are used to estimate the Direction Of Arrival (DOA) of an underwater acoustic signal source. These algorithms run inside the Master Unit's ODROID, and have two main parts. The first part consists of four sub-processes, which run in parallel with the main process, are initialized. These sub-processes are used to read the UDP packets sent from the four hydrophones (Hyd#1…Hyd#4). In this step, a first synchronization is carried out using a zero crossing detector of a reference counter inside each UDP packet. After that, the acquisition is started. Each sub-process generates groups of *N* UDP packets, corresponding to the sampling windows defined by the user. Finally, these groups are saved as a valid data in a FIFO queue, which is used to share information between parallel processes.

The second part is the reading at each iteration of one item from the four FIFO queues. Each of these signals has its own timestamp, therefore, a second synchronization is carried out to obtain a common timestamp. After that, each signal is filtered using a Band-Pass Filter (BPF) and compared with a minimum threshold. When all channels have a signal greater than the threshold and are

centred in the sampling windows, the signal is processed to estimate the TDOA and the DOA.

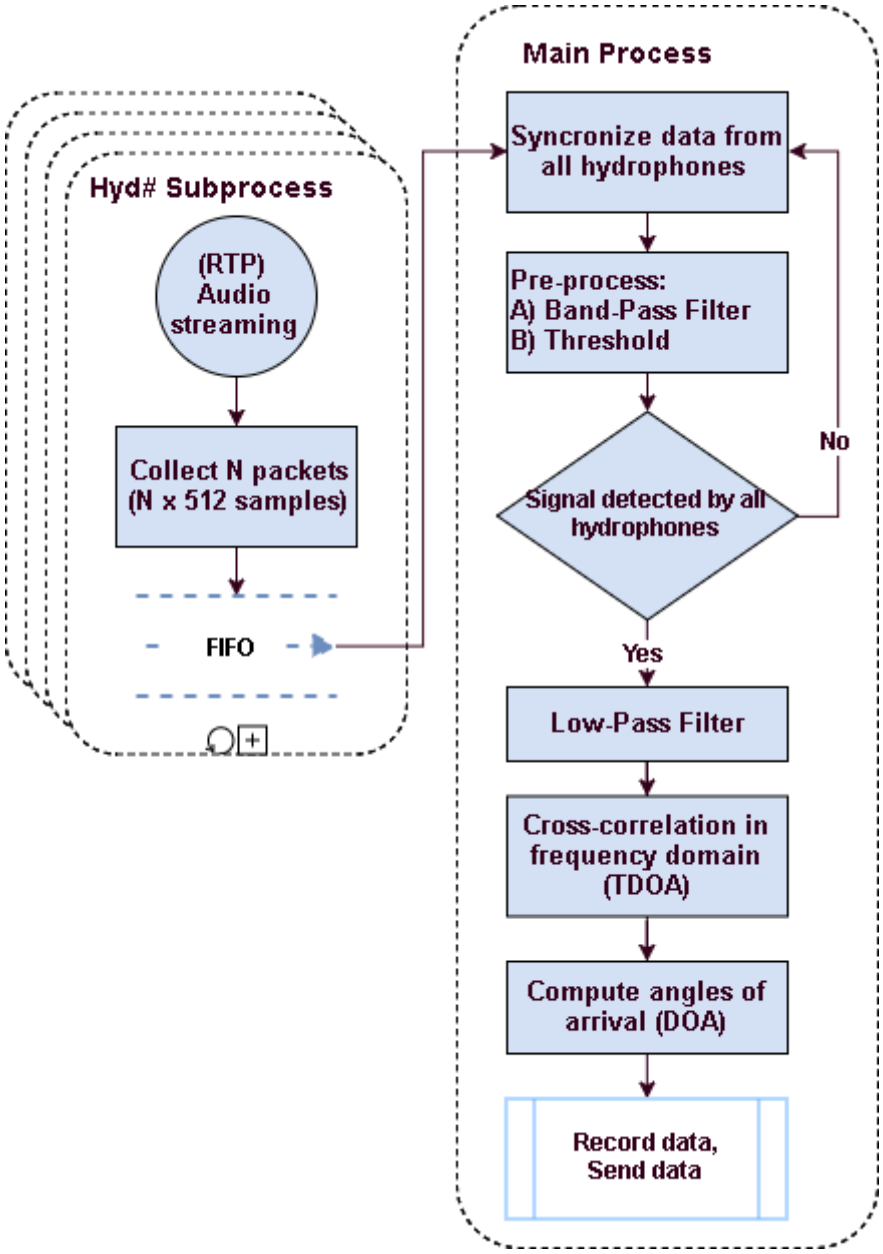

Figure 12 Block diagram of the algorithms used to compute the DOA of a sound source using the A2 hydrophones

The initial validation of the DOA algorithm has been done by performing four simulations with four virtual locations of a sound source (e.g. a boat) around the A2 array configuration described above. The simulations of the acquired signals by the 4 different hydrophones have been realized using a virtual location of a sound source, and then the time difference of sound arrival is calculated depending on the distance between the virtual sound source and the hydrophones. This delay is simulated by taking different audio signal slices with the corresponding delay in samples, and attenuation due to spherical divergence is calculated for each simulated signal. The output of the algorithm consists of the angle (Φ) between x-axis and the vector which defines the direction of arrival.

4. Results

4.1. A1 Hydrophone demonstration results

To demonstrate the end-to-end path from the A1 sensors to the web-based dissemination tool several real missions have been conducted in the Canary Islands (CAN), Norway (NOR) and Mediterranean (MED).

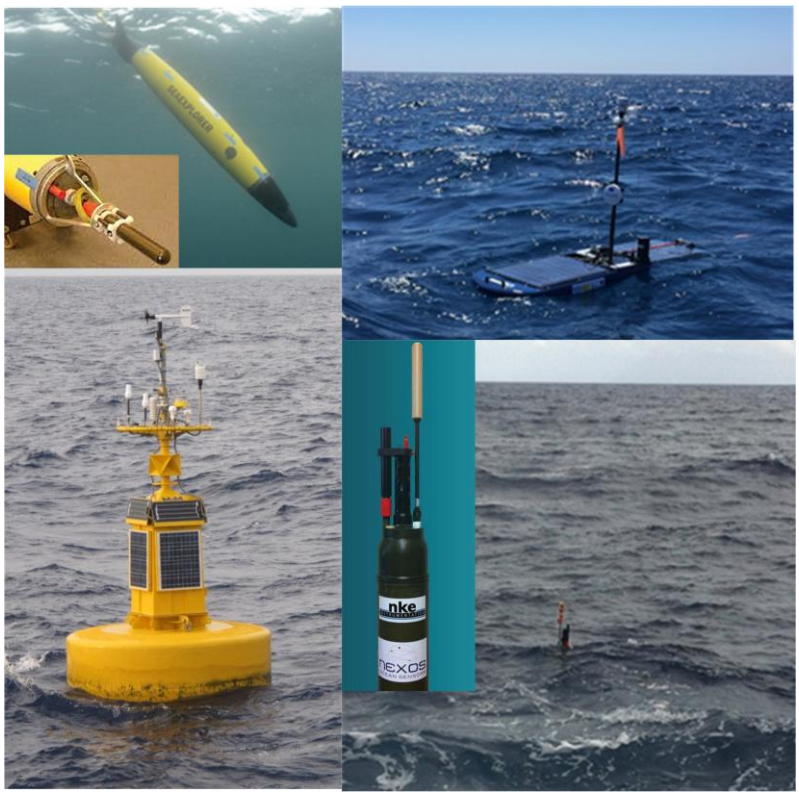

Figure 13 A1 hydrophone fully integrated in different platforms. Top-left deployment of SeaExplorer glider [25] (the A1 hydrophone in a metal bracket installed into the glider nose cone). Top-right deployment of Waveglider [(tow-body technical solution for the A1 hydrophone). Bottom-left deployment of A1 hydrophone in ESTOC-PLOCAN buoy. Bottom-right deployment of Provor float (assembly of A1 hydrophone on the top of float structure close to the CTD probe)

Five selected platforms were paired with A1 hydrophones (Figure 13) and tested in the mission sites as summarized in Table 3. These demonstration missions deal with assessing the effectiveness of integrating the A1 passive acoustics sensor into the different platforms with the purpose of monitoring the MSFD Indicator 11.2.1 continuous noise. In SeaExplorer glider, the A1 hydrophone was located in the glider's nose cone. In the Waveglider, the A1 hydrophone was located in the tow-body. In Provor float, the A1 hydrophone was located at the top of the float close to the CTD probe in order to measure data in the same water layer. The A1 was installed on the buoy platforms at a depth of about 5 m. Plots of recorded time series can be accessed via the NeXOS Sensor Web Visualization Server (http://www.nexosproject.eu/dissemination/sensor-web-visualization).

Table 3 Platforms and Sensors for each Demonstration Mission

Mission site	**Platform**	**Hydrophone type**	**Mission duration**
NOR (coast of Norway, near the island of Runde)	SEAEXPLORER GLIDER [30]	A1 with D/70	19th to 26th of June, 2017
CAN (East coast of Gran Canarias, offshore	WAVEGLIDER [31]	A1 with D/70	3rd to 9th of June, 2017

Taliarte)			
CAN (North-East coast of Gran Canarias, next to an aquaculture facility)	BUOY [32]	A1 with JS-B100	22nd of August to 14th of September, 2017
CAN (North-East coast of Gran Canarias)	PROVOR [33]	A1with SQ26-01	23rd to 24th of May, 2017
MED (1.2 nm offshore town of Senigallia, Italy)	BUOY [34]	A1 with JS-B100	20th of June to 16th of November, 2017

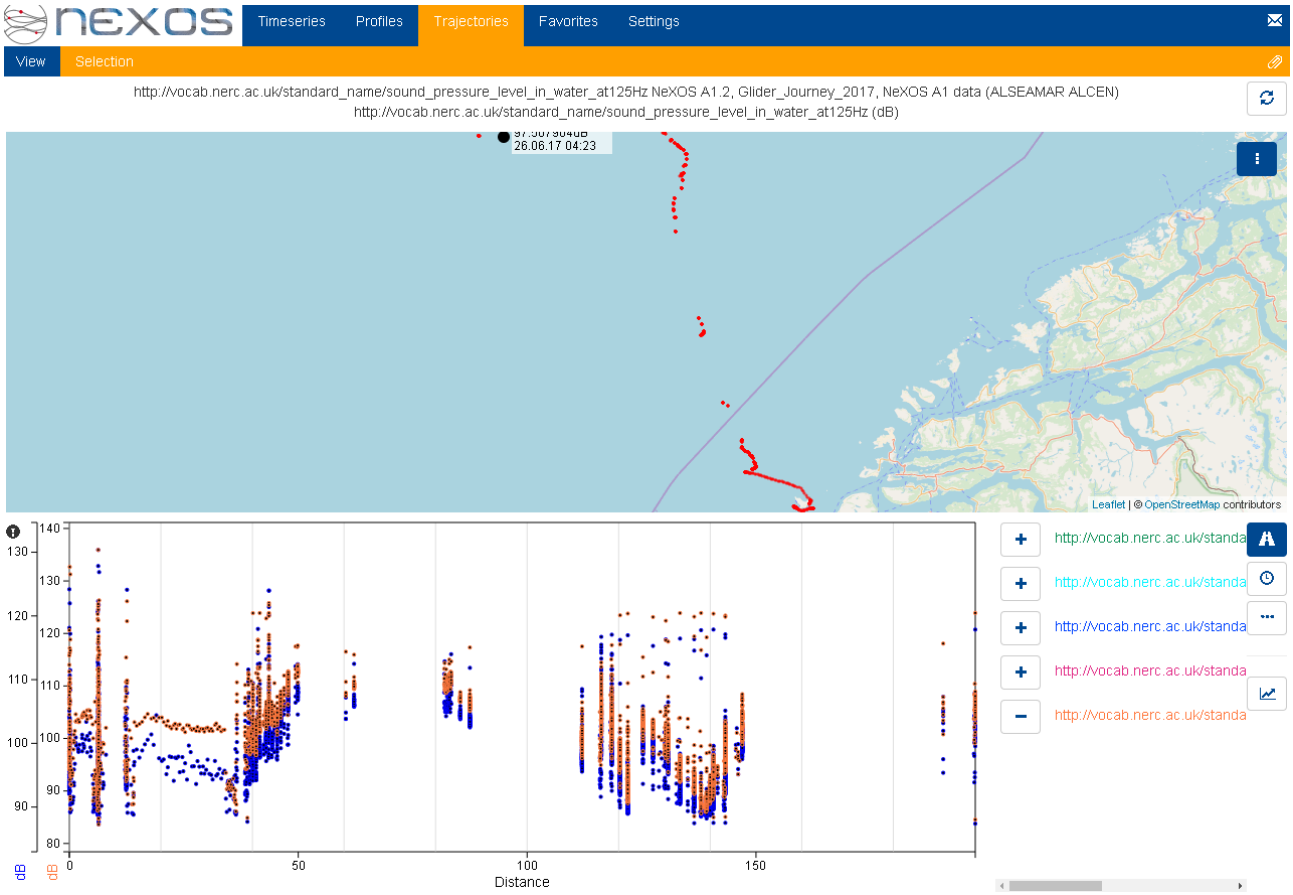

Figure 14 Time series of RMS sound pressure level in water for MSFD Indicator 11.2.1 (at 63 Hz - orange and 125 Hz - purple) in the coast of Norway, near the island of Runde, during the glider journey. The x-axis is data point number.

As shown in Figure 14 and with depth information available (though not displayed), the level of noise was shown to evolve with distance from the coast and depth. Spikes on the second half right of the graph are attributed to glider mechanics involved in the control of buoyancy. The highest solid peak in Figure 14 (about 45 to 90 km) is from the 17th to 19th of June. At this point the glider was near a popular fishing area. The overall level of noise (90-110 dB) is consistent with the level in the coast of Norway.

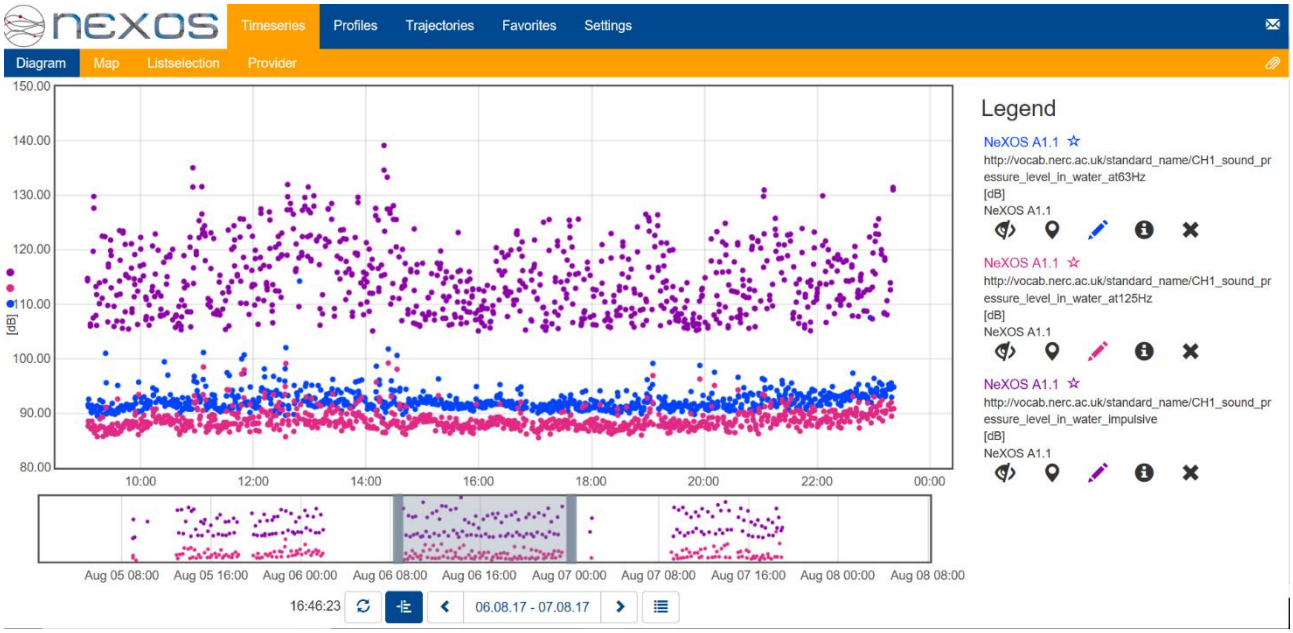

Figure 15 Time series of RMS sound pressure level in for MSFD Indicator 11.1.1 (purple) and MSFD Indicator 11.2.1 (at 63 Hz - blue and 125 Hz - red) in the coast of Gran Canaria, offshore Taliarte, during the Waveglider journey in August 6, 2017. The x-axis is time.

In the Waveglider mission, the calculated mean and standard deviation of the sound pressure level in water at 63 Hz is 92.3 dB and 2.0, and at 125 Hz is 88.7 dB and 1.8. The overall level of noise (88-92 dB) is consistent with the level along the coast of Gran Canarias, offshore Taliarte.

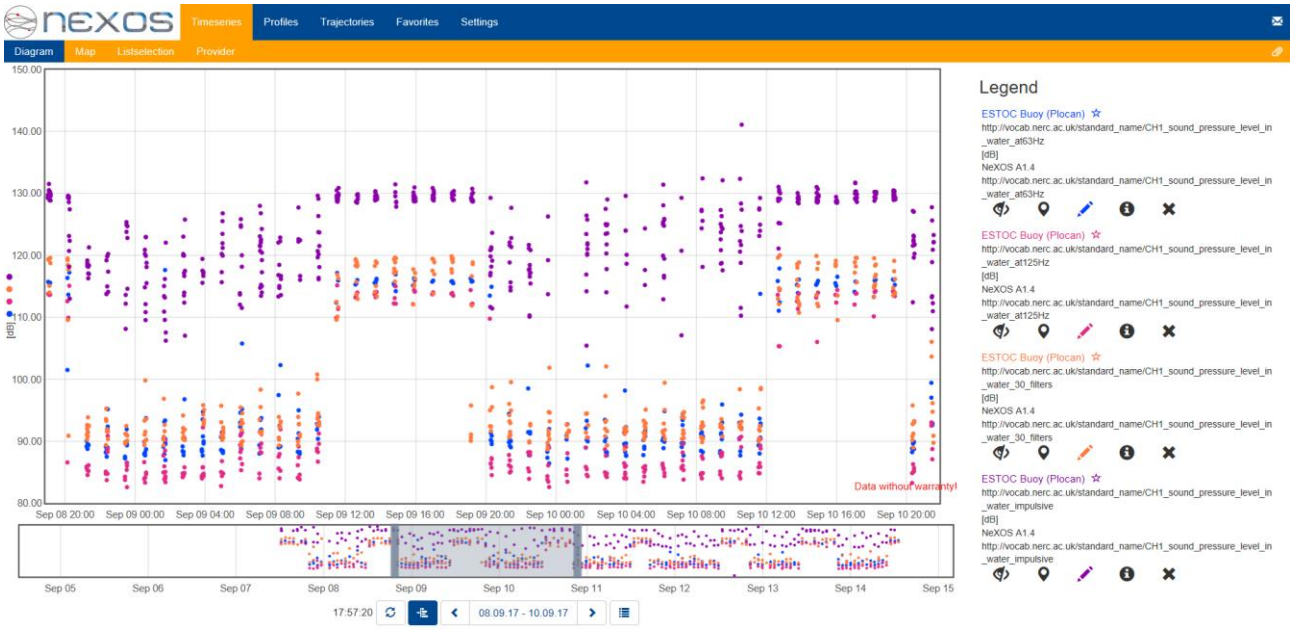

Figure 16 Time series of RMS sound pressure level in water for MSFD Indicator 11.1.1 (purple), MSFD Indicator 11.2.1 (at 63 Hz - blue and 125 Hz - red) and Extended MSFD Indicator 11.2.1 (orange), in the ESTOC site, starting from September 8 until September 11, 2017. The x-axis is time.

At the ESTOC site, the noise measurements display trends between day and night, probably correlated with ship traffic for aquaculture farm maintenance or harbour in-out traffic, as illustrated in Figure 16 (from September 8 until September 11, 2017). The calculated mean and standard deviation of the sound pressure level in water during the day (8:00 to 20:00) at 63 Hz is 106.3 dB and 11.9, and at 125 Hz is 102.7 dB and 12.9, and during the night (20:00 to 8:00) at 63 Hz is 90.9

dB and 4.4, and at 125 Hz is 85.9 dB and 2.2.

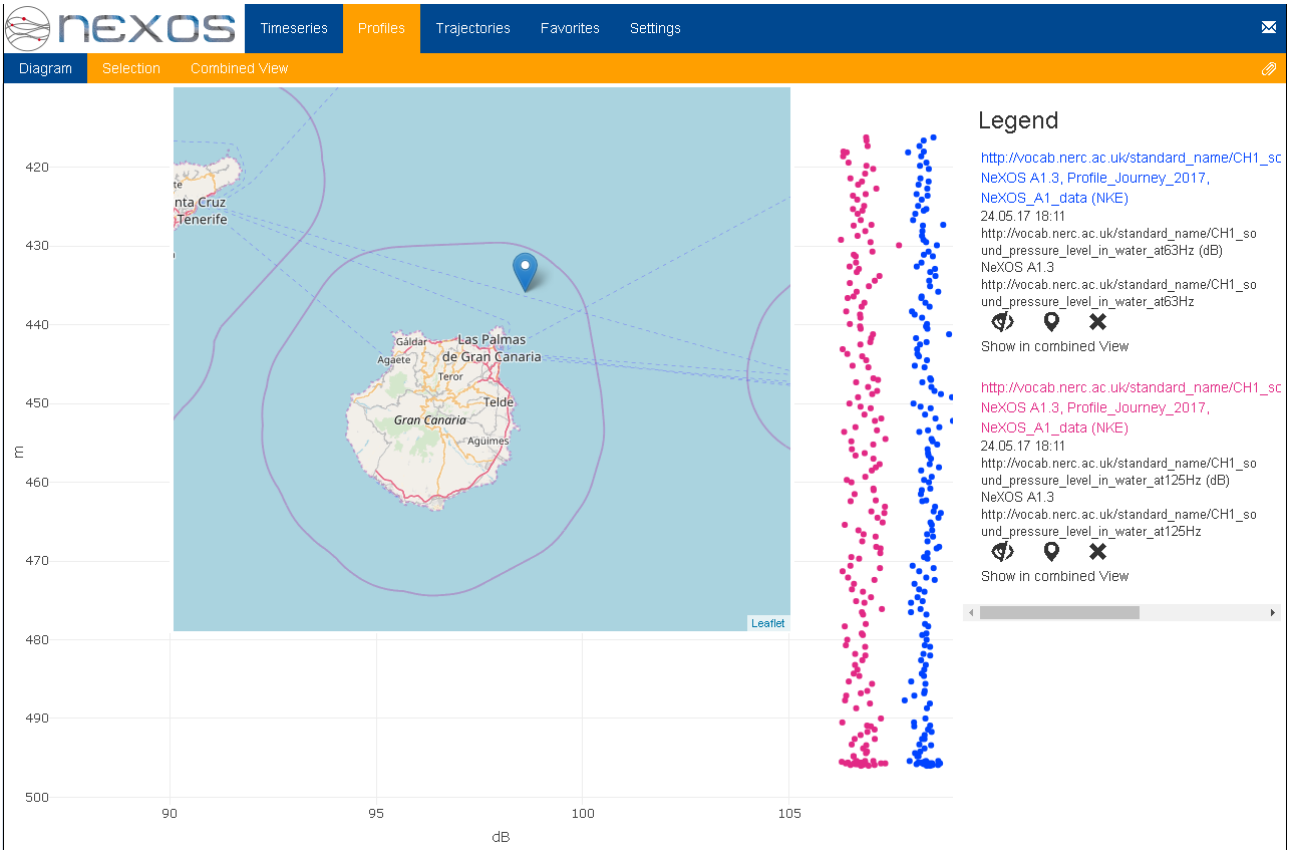

Figure 17 Time series of RMS sound pressure level in water for MSFD Indicator 11.2.1 (at 63 Hz - blue and 125 Hz - red) in the coast of Gran Canarias, during the float journey. The y-axis is depth.

A short mission was planned to check that the Provor float with the A1 hydrophone installed on it is fully functional. The float was programmed to achieve parking and profiling depths up to 500 meters and to monitor the overall noise level (MSFD Indicator 11.2.1) with the A1 hydrophone. The calculated mean and standard deviation of the sound pressure level in water at 63 Hz is 108.3 dB and 0.2, and at 125 Hz is 106.7 dB and 0.3.

Figure 18 Time series of RMS sound pressure level in water for MSFD Indicator 11.2.1 (at 63 Hz - blue and 125 Hz - red) in the TeleSenigallia site, starting from July 20 until July 24, 2017. The x-axis is date and time

At the TeleSenigallia site, the calculated mean and standard deviation of the sound pressure level in water at 63 Hz is 148.0 dB and 0.9, and at 125 Hz is 144.7 dB and 1.0. Therefore, this mission, has detected that these values are higher than expected (90-100 dB is a reference for the TeleSenigallia site) as the A1 signal processing algorithm did not correctly account for the actual sensitivity of the JSB100 hydrophone.

4.2. A2 Hydrophone demonstration results

To observe the performance of A2 hydrophone array configuration, a test was performed in the OBSEA observatory. In this test, an A2-centered 500m-radius circle track was performed using a boat equipped with a sound generator, allowing for a 360º assessment of performance of A2 DOA. Figure 19 illustrates one of the four A2 sensors deployed at OBSEA observatory.

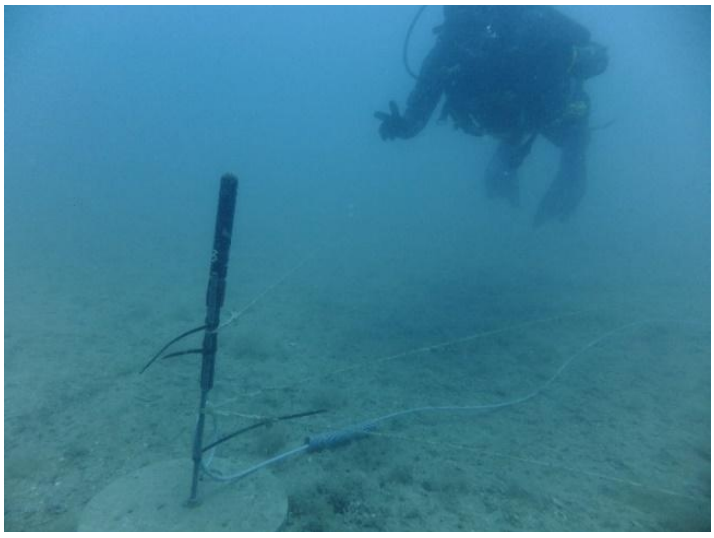

Figure 19 A2 sensor deployed for validation at OBSEA observatory

The computed DOA was sent to the SOS server. Moreover, a “True” angle between the A2 and the

boat was computed using a GPS, and was also sent to the SOS. These angles can be observed in Figure 20; the computed DOA is depicted in red and the "True" angle between the A2 and the boat, in blue.

Figure 20 A2 DOA vs GPS-measured of boat location, delivered to NeXOS SOS and viewed in the NeXOS SWE viewer

We can observe the error in a polar plot in Figure 21A. We can see that in some areas the error is much higher than others, creating a specific pattern, as is shown in [27]. In an estimation problem, where a set of noisy observations are used to estimate a certain parameter of interest, the Cramér-Rao Bound (CRB) sets the lowest bound on the covariance matrix that is asymptotically achievable by any unbiased estimation algorithm, and therefore its accuracy. The CRB is calculated from the inverse of the Fisher Information Matrix (FIM) $\mathbf{I}(\mathbf{p})$ of the *likelihood* function. Let the emitter location $\mathbf{p} \in \mathbb{R}^{\boldsymbol{n}}$ be the parameter of interest obtained from a vector of TDOAs measurements $\boldsymbol{z} = h(\mathbf{p}) + \boldsymbol{w} \in \mathbb{R}^{\boldsymbol{m}}$ where $\boldsymbol{w} \in \mathbb{R}^{\boldsymbol{m}}$ is zero mean Gaussian with covariance $\mathbf{R} \in \mathbb{R}^{\boldsymbol{m \times m}}$. Each entry of vector $h(\mathbf{p})$ has the form

$$h_{1j}(\mathbf{p}) = r_1(\mathbf{p}) - r_j(\mathbf{p}) = |\mathbf{p} - \mathbf{p_1}| - |\mathbf{p} - \mathbf{p_j}| \tag{8}$$

where the TDOAs have been taken between the reference sensor $\mathbf{p_1}$ and sensors $\mathbf{p_j}$ with $j = 2, \dots, m$. Due the Gaussian measurement noise, the *likelihood* function $p(z_{1j}|\mathbf{p})$ for a single TDOA measurement is given by

$$z_{1j} = h_{1j}(\mathbf{p}) + w \tag{9}$$

$$p(z_{1j}|\mathbf{p}) = \frac{1}{(2\pi)^{\frac{m}{2}}|\mathbf{R}|^{\frac{1}{2}}} exp\left\{-\frac{1}{2}\left(z_{1j} - h_{1j}(\mathbf{p})\right)^T \mathbf{R}^{-1}\left(z_{1j} - h_{1j}(\mathbf{p})\right)\right\} \tag{10}$$

And the gradient of the *log likelihood* function $p(z_{1j}|\mathbf{p})$ with respect to $\mathbf{p}$ computed as [28] results in an FIM equal to

$$\mathbf{I}(\mathbf{p}) = \nabla h_{1j}(\mathbf{p})^T \mathbf{R}^{-1} \nabla h_{1j}(\mathbf{p}) \tag{11}$$

is

$$\nabla h_{1j}(\mathbf{p}) = \frac{\partial h_{1j}(\mathbf{p})}{\partial \mathbf{p}} = \frac{1}{r_1(\mathbf{p})}(\mathbf{p} - \mathbf{p_1})^T - \frac{1}{r_j(\mathbf{p})}(\mathbf{p} - \mathbf{p_j})^T \tag{12}$$

which in matrix formulation can be described as

$$\nabla h(\mathbf{p}) = \begin{bmatrix} \nabla h_{1j}(\mathbf{p}) \\ \vdots \\ \nabla h_{1m}(\mathbf{p}) \end{bmatrix} = \frac{1}{r_1(\mathbf{p})}(\mathbf{p} - \mathbf{p_1})^T \begin{bmatrix} 1 & \dots & 0 \\ \vdots & \ddots & \vdots \\ 0 & \dots & 1 \end{bmatrix} - \begin{bmatrix} \frac{1}{r_j(\mathbf{p})} & \dots & 0 \\ \vdots & \ddots & \vdots \\ 0 & \dots & \frac{1}{r_m(\mathbf{p})} \end{bmatrix} \begin{bmatrix} (\mathbf{p} - \mathbf{p_j})^T \\ \vdots \\ (\mathbf{p} - \mathbf{p_m})^T \end{bmatrix} \tag{13}$$

Therefore, using (11) and (13) we can compute the CRB inequalities as follows. Suppose that $\hat{\mathbf{p}}$ is some unbiased estimator of the source of sound position that uses as observations the noisy TDOA measurements $\bar{\boldsymbol{z}}$ then

$$var\{\hat{\mathbf{p}}\} = E\{|\hat{\mathbf{p}}(\bar{\boldsymbol{z}}) - \mathbf{p}|^2\} \geq tr(\mathbf{I}(\mathbf{p})^{-1}) \tag{14}$$

Finally, a simulation using the FIM for a set of two TDOA measurements is calculated for a gird of possible emitter positions in the plane, which is shown in Figure 21B.

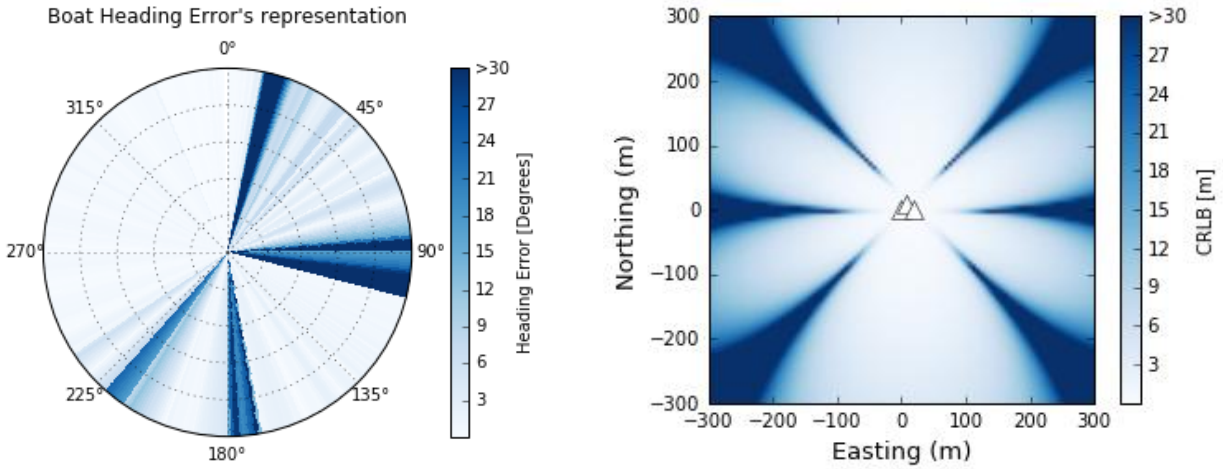

(A) (B)

Figure 21. A) Polar representation of heading error, considering Boat representation. B) CRB of TDOA scenario

Figure 21B shows the expected pattern of the accuracy of the source localization algorithm through the CRB, which can be compared with the real error obtained during the field test, Figure 21A. A standard deviation equal to $1\mu s$ was used for the simulation. In this scenario, both simulation and field test have similar values, which have an error lower than 3 m on the good areas and errors around 30 m in the worst cases. On the other hand, the differences between them can be due to the accuracy of the hydrophones' position during their deployment.

5. Conclusions

Two compact low power (A1 has a power consumption < 1W and A2 has approximately 1.1 W), low-noise digital hydrophone systems with embedded processing, A1 and A2, were developed by the NeXOS project team. The embedded functions developed for these innovative sensors are:

- Noise statistics (including EU MSFD Indicators)
- Mammal detection (PAMguard)
- Directional sound source information
- Storage of relevant raw data in internal memory.

The A1 and A2 acoustic systems are designed for mobile platforms such as Gliders / AUVs and can also equip larger platforms such as deep fixed observing systems. All the embedded algorithms have been evaluated in different laboratory tests and validated in real missions using different platforms such as SeaExplorer glider, PROVOR float, ESTOC buoy to monitor noise and OBSEA cable observatory to determine the direction of a sound source. Monitoring of trends in the ambient noise level within the 1/3 octave bands of 63 and 125 Hz (centre frequency) using all these different platforms equipped with A1 acoustic systems has been successful except at the TeleSenigallia site. In this case it has been identified that the signal processing algorithm did not correctly account for the actual sensitivity of the JSB100 hydrophone.

Finally, we can conclude that A2 estimates fit reasonably well with the actual sound generator location and therefore the result of this test was successful, partly validating by /demonstrating, the capability of A2 to estimate. The DOA estimations with A2, tested at OBSEA observatory, have similar values to the simulation tests, presenting errors lower than 3 m on the good areas and errors around 30 m in the worst cases. Moreover, the differences between the field test estimations and the simulations can be due to the accuracy of the hydrophones' position during their deployment. More experiments would be needed for further validation in different scenarios (changing landscape, robustness vs background noise, etc.), not achievable within the limited resources of the project for field work. Also, though possible in theory, the presented A2 system is not yet capable to estimate the source distance. However, early simulations indicate that it would be possible to estimate both the DOA and the source distance of acoustic tags.

Acknowledgment

NeXOS is a collaborative project funded by the European Commission 7th Framework Programme, under the call OCEAN-2013.2 - The Ocean of Tomorrow 2013 – Innovative multifunctional sensors for in-situ monitoring of marine environment and related maritime activities (grant agreement No 614102). It is composed of 21 partners including SMEs, companies and scientific organizations from 6 European countries. This work was partially supported by the project JERICO-NEXT from the European Commission's Horizon 2020 research and Innovation program under Grant Agreement No. 654410.

References

[1] E. C. Directive, "56/EC of the European Parliament and of the Council of 17 June 2008 establishing a framework for community action in the field of marine environmental policy (Marine Strategy Framework Directive)," *Off. J. Eur. Union*, vol. 164, pp. 19–40, 2008.

[2] Clark, C. W., Ellison, W. T., Southall, B. L., Hatch, L., Van Parijs, S. M., Frankel, A., & Ponirakis, D. (2009). Acoustic masking in marine ecosystems: intuitions, analysis and implication. Mar. Ecol.-Prog. Ser., vol. 395, pp. 201-222

[3] J. Pearlman et al., "Requirements and approaches for a more cost-efficient assessment of ocean

waters and ecosystems, and fisheries management," 2014 Oceans - St. John's, St. John's, NL, 2014, pp. 1-9. doi: 10.1109/OCEANS.2014.7003144
[4] T. J. Olmstead, M. A. Roch, P. Hursky, M. B. Porter, H. Klinck, D. K. Mellinger, T. Helble, S. S. Wiggins, G. L. D'Spain, and J. A. Hildebrand, "Autonomous underwater glider based embedded real-time marine mammal detection and classification," The Journal of the Acoustical Society of America, vol. 127, p. 1971, 2010.
[5] Peter H.J. Porskamp, Jeremy E. Broome, Brian G. Sanderson and Anna M. Redden. "Assessing the Performance of Passive Acoustic Monitoring Technologies for Porpoise Detection in a High Flow Tidal Energy Test Site". Journal of the Canadian Acoustical Association, vol 43, No 3, 2015.
[6] E. Delory, D. Toma, J. Del Rio, P. Ruiz, and L. Corradino, “NeXOS objectives in multi-platform underwater passive acoustics.”
[7] I. S. Association and others, “Standard for a Precision Clock Synchronization Protocol for Networked Measurement and Control Systems,” *IEEE 1588*, 2002.
[8] A. Bröring, J. Echterhoff, S. Jirka, I. Simonis, T. Everding, C. Stasch, S. Liang, and R. Lemmens, “New generation Sensor Web Enablement,” *Sensors*, vol. 11, no. 3, pp. 2652–2699, 2011.
[9] D. M. Toma, J. Del Rio, S. Jirka, E. Delory, J. Pearlman, and C. Waldmann, “NeXOS smart electronic interface for sensor interoperability,” in *MTS/IEEE OCEANS 2015: Discovering Sustainable Ocean Energy for a New World, Genova, Italy, May 18-21*, 2015.
[10] T. O’Reilly, “OGC® PUCK Protocol Standard Version 1.4,” Wayland, MA, 01778, USA, 2012.
[11] M. Botts and A. Robin, “OGC SensorML: Model and XML Encoding Standard,” Wayland, MA, 01778, USA, 2014.
[12] E. Martinez, D. M. Toma, S. Jirka, and J. Del R’\io, “Middleware for Plug and Play Integration of Heterogeneous Sensor Resources into the Sensor Web,” *Sensors*, vol. 17, no. 12, p. 2923, 2017.
[13] J. Pearlman, S. Jirka, J. del Rio, E. Delory, L. Frommhold, S. Martinez, and T. O’Reilly, “Oceans of Tomorrow sensor interoperability for in-situ ocean monitoring,” in *OCEANS 2016 MTS/IEEE Monterey*, 2016, pp. 1–8.
[14] J. Del Rio, D. M. Toma, T. C. O’Reilly, A. Broring, D. R. Dana, F. Bache, K. L. Headley, A. Manuel-Lazaro, and D. R. Edgington, “Standards-based plug & work for instruments in ocean observing systems,” *IEEE J. Ocean. Eng.*, vol. 39, no. 3, pp. 430–443, 2014.
[15] S. Memè, E. Delory, J. Del Rio, S. Jirka, D. M. Toma, E. Martinez, L. Frommhold, C. Barrera, and J. Pearlman, “Efficient Sensor Integration on Platforms (NeXOS),” in *AGU Fall Meeting Abstracts*, 2016.
[16] J. del Rio, D. M. Toma, E. Mart’\inez, T. C. O’Reilly, E. Delory, J. S. Pearlman, C. Waldmann, and S. Jirka, “A Sensor Web Architecture for Integrating Smart Oceanographic Sensors into the Semantic Sensor Web,” *IEEE J. Ocean. Eng.*, 2017.
[17] S. Zaugg, M. van der Schaar, L. Houégnigan, and M. André, “A framework for the automated real-time detection of short tonal sounds from ocean observatories,” *Appl. Acoust.*, vol. 73, no. 3, pp. 281–290, 2012.
[18] D. René, T. Mark, V. D. G. Sandra, A. Michael, A. Mathias, A. Michel, B. Karsten, C. Manuel, C. Donal, D. John, F. Thomas, L. Russell, P. Jukka, R. Paula, R. Stephen, S. Peter, S. Gerry, T. Frank, W. Stefanie, W. Dietrich, and Y. John, *Monitoring Guidance for Underwater Noise in European Seas- Part II: Monitoring Guidance Specifications*. 2014.
[19] A. J. der Graaf, M. A. Ainslie, M. André, K. Brensing, J. Dalen, R. P. A. Dekeling, S.

Robinson, M. L. Tasker, F. Thomsen, and S. Werner, “European Marine Strategy Framework Directive-Good Environmental Status (MSFD GES): Report of the Technical Subgroup on Underwater noise and other forms of energy,” *Brussels*, 2012.
[20] I. E. Commission and others, *Electroacoustics: Octave-band and Fractional-octave-band Filters*. IEC, 1995.
[21] D. Gillespie, D. K. Mellinger, J. Gordon, D. Mclaren, P. Redmond, R. McHugh, P. W. Trinder, X. Y. Deng, and A. Thode, “PAMGUARD: Semiautomated, open source software for real-time acoustic detection and localisation of cetaceans,” *J. Acoust. Soc. Am.*, vol. 30, no. 5, pp. 54–62, 2008.
[22] J.-M. Valin, F. Michaud, J. Rouat, and D. Létourneau, “Robust sound source localization using a microphone array on a mobile robot,” in *Intelligent Robots and Systems, 2003.(IROS 2003). Proceedings. 2003 IEEE/RSJ International Conference on*, 2003, vol. 2, pp. 1228–1233.
[23] A. Nehorai and E. Paldi, “Acoustic vector-sensor array processing,” *IEEE Trans. signal Process.*, vol. 42, no. 9, pp. 2481–2491, 1994.
[24] L. C. Godara, “Application of antenna arrays to mobile communications. II. Beam-forming and direction-of-arrival considerations,” *Proc. IEEE*, vol. 85, no. 8, pp. 1195–1245, 1997.
[25] J. Benesty, J. Chen, and Y. Huang, “Direction-of-Arrival and Time-Difference-of-Arrival estimation,” *Microphone Array Signal Process.*, pp. 181–215, 2008.
[26] Â. M. C. R. Borzino, J. A. Apolinário Jr, and M. L. R. de Campos, “Consistent DOA estimation of heavily noisy gunshot signals using a microphone array,” *IET Radar, Sonar Navig.*, vol. 10, no. 9, pp. 1519–1527, 2016.
[27] R. Kaune, J. Hörst, and W. Koch, “Accuracy analysis for TDOA localization in sensor networks,” in *Information Fusion (FUSION), 2011 Proceedings of the 14th International Conference on*, 2011, pp. 1–8.
[28] A. Alcocer. “Positioning and Navigation Systems for Robotic Underwater Vehicles,” PhD thesis, Universidade Tecnica de Lisboa Instituto Superior Tecnico, 2009.
[29] ANSI S12.9-2005, Quantities and Procedures for Description and Measurement of Environmental Sound
[30] https://www.alseamar-alcen.com/products/underwater-glider/seaexplorer
[31] https://www.liquid-robotics.com
[32] http://siboy.plocan.eu
[33] http://www.nke-instrumentation.com/products/profilers/products/provor-cts4.html
[34] http://rmm.an.ismar.cnr.it/index.php/meda-senigallia